Earth and Planetary Science Letters 399 (2014) 1–13

Contents lists available at ScienceDirect

Earth and Planetary Science Letters

www.elsevier.com/locate/epsl

Incursion of meteoric waters into the ductile regime in an active orogen

Catriona D. Menzies [a,*], Damon A.H. Teagle [a], Dave Craw [b], Simon C. Cox [c], Adrian J. Boyce [d], Craig D. Barrie [d,e], Stephen Roberts [a]

[a] Ocean and Earth Science, National Oceanography Centre Southampton, University of Southampton, Southampton SO14 3ZH, UK
[b] Department of Geology, University of Otago, Dunedin, New Zealand
[c] GNS Science, Private Bag 1930, Dunedin 9054, New Zealand
[d] S.U.E.R.C., Scottish Enterprise Technology Park, Rankine Avenue, East Kilbride, Glasgow G75 0QF, UK
[e] Isoprime Ltd., Isoprime House, Earl Road, Cheadle Hulme, Cheadle SK8 6PT, UK

ARTICLE INFO

Article history:
Received 21 September 2013
Received in revised form 14 March 2014
Accepted 29 April 2014
Available online xxxx
Editor: T. Elliott

Keywords:
fluid flow
stable isotopes
Alpine Fault
fluid inclusions
Southern Alps
meteoric water

ABSTRACT

Rapid tectonic uplift on the Alpine Fault, New Zealand, elevates topography, regional geothermal gradients, and the depth to the brittle ductile transition, and drives fluid flow that influences deformation and mineralisation within the orogen. Oxygen and hydrogen stable isotopes, fluid inclusion and Fourier Transform Infrared (FT-IR) analyses of quartz from veins which formed at a wide range of depths, temperatures and deformation regimes identify fluid sources and the depth of penetration of meteoric waters. Most veins formed under brittle conditions and with isotope signatures ($\delta^{18}O_{H_2O} = -9.0$ to $+8.7‰_{VSMOW}$ and $\delta D = -73$ to $-45‰_{VSMOW}$) indicative of progressively rock-equilibrated meteoric waters. Two generations of quartz veins that post-date mylonitic foliation but endured further ductile deformation, and hence formation below the brittle to ductile transition zone (>6–8 km depth), preserve included hydrothermal fluids with δD values between −84 and −52‰, indicating formation from meteoric waters. FT-IR analyses of these veins show no evidence of structural hydrogen release, precluding this as a source of low δD values. In contrast, the oxygen isotopic signal of these fluids has almost completely equilibrated with host rocks ($\delta^{18}O_{H_2O} = +2.3$ to $+8.7‰$). These data show that meteoric waters dominate the fluid phase in the rocks, and there is no stable isotopic requirement for the presence of metamorphic fluids during the precipitation of ductilely deformed quartz veins. This requires the penetration during orogenesis of meteoric waters into and possibly below the brittle to ductile transition zone.

1. Introduction

Fluids play a key role in orogenesis through the transport of heat and mass (Bickle and McKenzie, 1987), by changing the rheological behaviour of rocks and localising deformation (Wintsch et al., 1995), and concentrating valuable mineral resources (Weatherley and Henley, 2013). The impact of fluids on mountain building depends on fluid sources, flow paths and temperatures, and extent of fluid–rock interaction at different crustal levels (Yardley, 2009).

Orogenic fluids originate from a variety of sources. During metamorphism fluids are generated by prograde metamorphic devolatilisation reactions and by the release of water during the crystallisation of partial melts (Norris and Henley, 1976; Walther and Orville, 1982; Yardley, 2009, 1997). In some orogenic belts mantle derived fluids (Kennedy and van Soest, 2007) or fluids liberated from igneous intrusions (Burrows et al., 1986; Reynolds and Lister, 1987) play key roles and have been inferred as carriers of gold in Archean shear zones (Groves, 1993). The high relief of collisional mountain belts provides strong driving forces for the deep penetration of meteoric fluids (Barker et al., 2000; Chamberlain et al., 1995; Koons and Craw, 1991) and the brittle upper crust is expected to be saturated with surface-derived waters. However, the relative contributions of different fluid sources remains poorly quantified. In particular, whether meteoric fluids can penetrate beyond the brittle regime into ductilely deforming rocks remains controversial and conceptually challenging (e.g. Connolly and Podladchikov, 2004). Oxygen and hydrogen isotope measurements of minerals and veins from ancient crustal shear zones have been presented as evidence for penetration of meteoric fluids to depths of 5 to 18 km

* Corresponding author. Tel.: +44 2380 596539.
E-mail address: c.menzies@soton.ac.uk (C.D. Menzies).

http://dx.doi.org/10.1016/j.epsl.2014.04.046

(Barker et al., 2000; Clark et al., 2006; Fricke et al., 1992; McCaig et al., 1990; Raimondo et al., 2011). However, low $\delta^{18}O$ and δD signatures resulting from near surface alteration prior to burial can be retained in some orogens (Raimondo et al., 2013). Assuming water–rock isotopic equilibrium the high proportion of oxygen in both water and rocks means that "rock dominated" fluid signatures are developed at relatively low water–rock ratios, as expected within or below the brittle to ductile transition zone (BDTZ) where large permeability and porosity and high fluid fluxes are problematic (e.g. Connolly and Podladchikov, 2004 and Fusseis et al., 2009). This means that evolved meteoric fluids have oxygen isotopic signatures that are indistinguishable from metamorphic fluids. Although fractionation equations between hydrous minerals and water are poorly calibrated (Graham et al., 1987), because hydrogen is relatively more abundant in water than in rocks, it provides a more enduring tracer of fluid origins. As such meteoric waters will only attain hydrogen isotopic signatures similar to metamorphic rocks at very low water–rock ratios ($w/r = 0.001$).

To investigate the depth of penetration of meteoric waters we have examined the Southern Alps of New Zealand, an active orogen where uplift rates and depths of formation of hydrothermal veins are well constrained and there is no evidence of syn-orogenic magmatic activity. This study uses oxygen and hydrogen stable isotope analyses of quartz, chlorite and adularia vein minerals to examine fluid flow from near surface to the middle crust. Our study focuses on measurements of δD in fluid inclusions from ductilely deformed veins, providing direct measurements of fluids that formed veins down to the ductile regime.

1.1. Geological setting

Oblique convergence of 39.7 ± 0.7 mm/yr (DeMets et al., 2010) between the Pacific and Australian plates through South Island, New Zealand (Fig. 1a) has caused crustal thickening and this, influenced by orographic rainfall and high erosion rates, has built the >3000 m high Southern Alps. Through the South Island the plate boundary is marked by the Alpine Fault which has recorded ~470 km of dextral strike slip motion since the Miocene (Cox and Sutherland, 2007; Sutherland, 1999). Rapid uplift of up to 10 mm/yr (Norris and Cooper, 2007) has exhumed lower crustal rocks in the hangingwall adjacent to the Alpine Fault. Uplift rates decrease towards the south east, where rocks from progressively shallower crustal depths crop out exposing a ~25 km crustal section (Cox and Barrell, 2007). The hangingwall of the Alpine Fault is composed of quartzofeldspathic metasediments and minor metavolcanic units of the Alpine Schists, with the highest metamorphic grade schists (garnet–oligoclase zone amphibolite facies) exhumed adjacent to the Alpine Fault (Cox and Barrell, 2007). These rocks are thrust over Cambrian to Early Ordovician Greenland Group metasediments and Devonian to Carboniferous and Cretaceous intrusives of the Australian Plate (Cox and Barrell, 2007).

The study area encompasses the highest uplift region where geothermal gradients are elevated due to rapid uplift and high rates of erosion (Koons, 1989). The depth of the BDTZ is estimated based on geothermal gradients and the base of the seismogenic crust. A geothermal gradient of $62.6 \pm 2.1\,^{\circ}C/km$ was measured in a ~150 m borehole adjacent to the Alpine Fault (Sutherland et al., 2012), which is similar to an estimate of $\sim 75\,^{\circ}C/km$ based on fluid inclusion studies (Craw, 1997). These geothermal gradients indicate that the 300 °C isotherm, which corresponds to the approximate onset of brittle–ductile deformation in quartzofeldspathic rocks (Stockhert et al., 1999), is at ~5 km depth. The true depth may be greater than this estimate as the geothermal gradient may decrease with depth in the crust (Koons, 1987). Regionally few earthquakes occur below 10–12 km depth in the Southern Alps and in the highest uplift region the base of seismogenesis is 3–4 km shallower (Leitner et al., 2001). Taken together, this evidence suggests that the BDTZ is 6–8 km deep in the study area (Fig. 1c).

Highly altered, cataclastic brittle fault rocks crop out directly adjacent to the Alpine Fault, but ~25 to 50 m structurally above these, mylonitic schists showing little near-surface alteration occur for ~1000 m. Both brittle and ductile fault rocks show evidence of fluid–rock exchange and mineral precipitation during deformation. Fluid–rock interaction under ductile conditions is preserved by synkinematic ductilely deformed quartz veins (Toy et al., 2010). Fault rocks deformed in a brittle manner are highly altered and retrogressed to green, clay-rich cataclasite (Warr and Cox, 2001). The presence of ductilely deformed veins, brittle veins, and hydrothermal mineral alteration assemblages suggest that fluids are present in the fault zone from below the BDTZ (>6–8 km) to the surface.

Warm springs emanate from 1 to 20 km south east of the Alpine Fault. Stable isotope signatures of these springs (Barnes et al., 1978; Reyes et al., 2010) and veins (Horton et al., 2003; Jenkin et al., 1994) in the Southern Alps have identified that meteoric waters are the dominant fluid in the upper ~2 km of the crust. At >2 km depth in the brittle crust of the Inboard zone (Fig. 1b) fluid inclusion and stable isotope studies of vein minerals indicate hydrothermal fluids were of relatively low salinity (~2–5 wt.% NaCl equivalent, Craw, 1988), had partially rock-equilibrated meteoric $\delta^{18}O$ values ($\delta^{18}O_{H_2O} = -0.7$ to 8.5‰, Horton et al., 2003; Jenkin et al., 1994; Koons et al., 1998), and δD values also indicative of a meteoric origin ($\delta D_{H_2O} = -29$ to -68‰, Jenkin et al., 1994). In samples from the Main Divide zone (Fig. 1b), fluid inclusions are more saline (up to 18 wt.%, Craw, 1988) and oxygen isotope data indicates that waters circulating at more than ~2 km depth (Craw et al., 1987) are in oxygen isotopic equilibrium with host rocks ($\delta^{18}O_{H_2O} > 5$‰, Craw, 1988; Koons et al., 1998). These fluids may therefore be deeply circulating rock-buffered meteoric waters or expelled mid-crustal metamorphic fluids (Craw, 1988; Craw et al., 1987; Horton et al., 2003; Koons et al., 1998; Templeton et al., 1998). δD values of vein generations that formed under ductile conditions have not been measured previously.

1.2. Sample descriptions

Vein samples representative of mineral precipitation over a range of conditions into the ductile regime (>6–8 km depth) were taken from the Inboard and Main Divide zones of the Southern Alps (Figs. 1a and b and Table 1). The deepest formed veins display evidence of folding or deformation-induced recrystallisation of vein minerals (Toy et al., 2010). Two types of ductilely deformed veins from the Alpine Fault zone (AFZ) were analysed:

Foliation Parallel and Foliation Boundinage veins: (Types (i) and (iii), Toy et al., 2010). Additionally one sample of a Foliation Parallel vein from Chancellor Dome, ~8 km south east of the Alpine Fault (Wightman et al., 2006), was analysed. Veins are composed of quartz ± calcite ± chlorite, but these minerals may not be in textural equilibrium. Veins cross cut mylonitic foliation (see Fig. 7, Toy et al., 2010) and are further ductilely deformed, as shown by quartz and calcite grain microstructures which are indicative of ductile deformation (see Fig. S1 in the Supplementary Materials). Foliation Parallel veins are 0.5 to 2 cm wide and are more strongly deformed at higher temperatures and record fluid flow at deeper crustal levels than the 0.5 to 4 cm wide Foliation Boudinage veins. All other veins sampled were formed within the brittle crust (at depths of <6 km).

FZ Fissure veins: (Type (iv), Toy et al., 2010). These veins occur only in the Alpine Fault zone. They cross cut the mylonitic foliation and show evidence for limited ductile deformation indicating

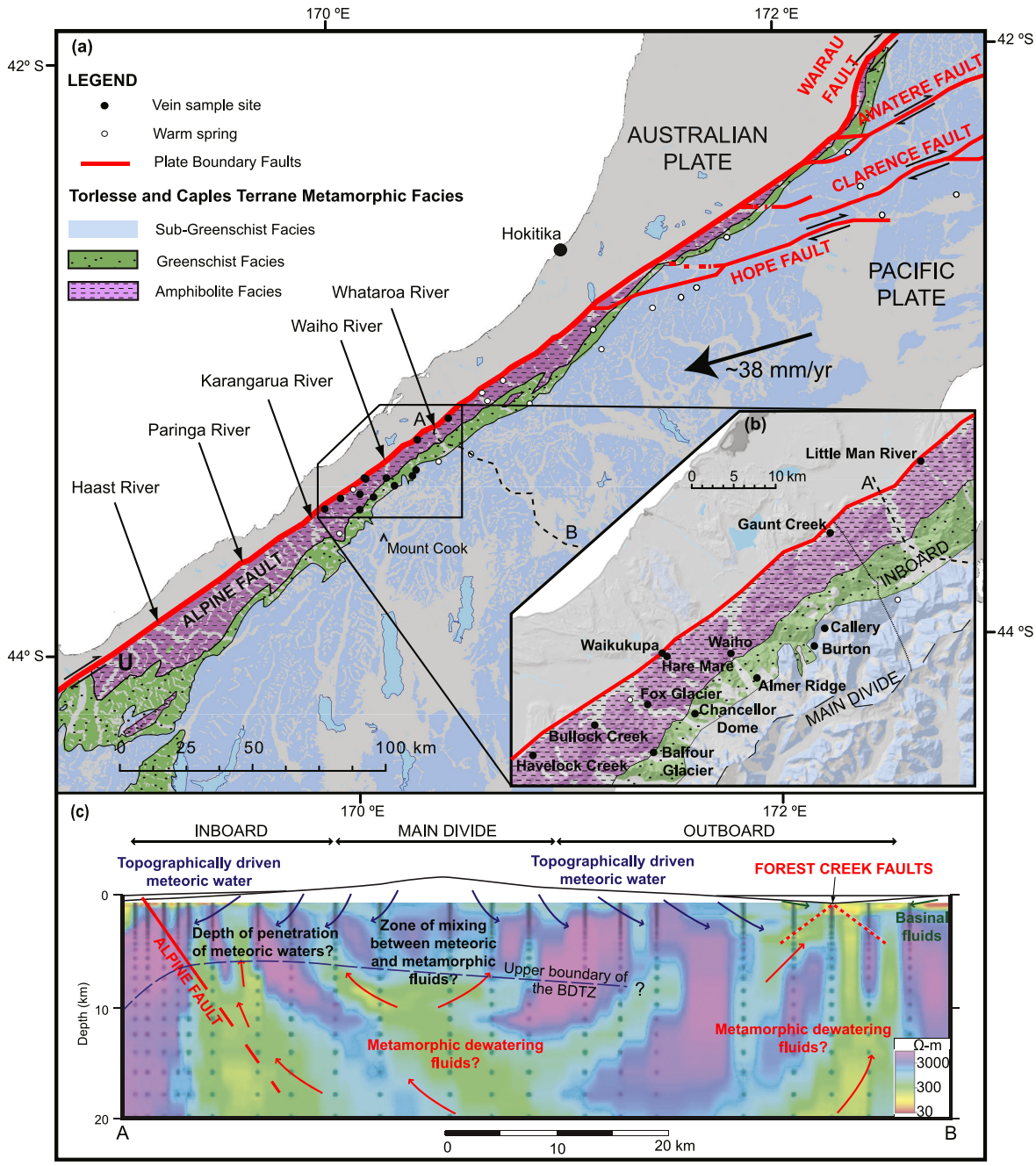

Fig. 1. (a) and (b) Tectonic map of central South Island, New Zealand, showing vein sampling localities, warm springs and metamorphic facies. The SIGHT transect line is also shown marked by a dashed line A to B. (c) Cross section of the central Southern Alps along the SIGHT line A to B. Shading represents conductive zones in the crust which may indicate the presence of water (resistivity model of Wannamaker et al., 2002) and fluid flow regimes are summarised from Barnes et al. (1978); Craw and Campbell (2004); Horton et al. (2003); Jenkin et al. (1994); Reyes et al. (2010); Templeton et al. (1998); Upton et al. (2003, 1995). The Inboard, Main Divide and Outboard tectonic zones and the estimated upper limit of the brittle to ductile transition zone (BDTZ) are shown.

they formed near the BDTZ. They are 0.5 to 2 cm wide and are composed of quartz ± calcite ± chlorite ± pyrite.

Joint Coating veins: Mineralised joints cross cut earlier, deeper-formed brittle structures which host FZ Fissure veins in the AFZ and are inferred to record fluid flow at shallow levels (<2 km). These millimetre-thick crusts on joint surfaces are composed of quartz ± calcite ± chlorite.

Inboard Fissure veins: At 5 to 10 km south east from the Alpine Fault, but still within the Inboard zone, fluid flow is recorded by Fissure veins which are typically up to 10 cm wide and commonly contain open space filled prismatic quartz crystals up to 5 cm (Craw, 1988). These veins are composed of quartz ± calcite ± chlorite ± adularia ± muscovite ± pyrite (Craw et al., 1994; Craw, 1988; Jenkin et al., 1994; Holm et al., 1989; Teagle et al., 1998).

Main Divide veins: These vein sets are associated with gold mineralisation near the Main Divide and have been sampled in the Upper Callery River and the Burton Glacier (Figs. 1a and b). Veins typically >10 cm wide infill fractures, joints and irregular cavities in wall rock and are principally composed of quartz ± calcite with minor adularia ± chlorite ± mica ± sulfides and rare gold (Craw et al., 1987, 2009) (Table 1).

2. Methods

Prior to stable isotope analysis vein samples underwent detailed hand specimen and petrographic description; fluid inclusion

Table 1
Summary of sampled vein types. Vein types from each location are listed in order of formation; earliest to latest. AFZ = Alpine Fault zone; AF = Alpine Fault; IN = Inboard zone; MD = Main Divide zone; Qtz = Quartz; CC = Calcite; Chl = Chlorite; Ad = Adularia; Mus = Muscovite; Bt = Biotite; Ars = Arsenopyrite; Gal = Galena; Au = Gold; Pyt = Pyrite; St = Stibnite; MB = Metabasic; QFS = Quartzofeldspathic.

	Location	Depth (km)	Dist. AF	Host rock	Structural setting	Vein minerals	Vein width	Previous works	Other Names
Joint Coatings	AFZ	Shallow (>3)	<1 km	Ampibolite Facies Mylonites & Cataclasites	Coating on joint surfaces	CC±Qtz±Chl±Pyt	sub-mm		
FZ Fissure	AFZ	Above BDTZ (<6)	<1 km	Amphibolite Facies QF and MB Mylonite	Open filling of fractures	Qtz±CC±Chl	0.5–2 cm	Toy et al. (2010)	Type iv
Foliation Boudinage	AFZ	BDTZ (~6)	<1 km	Amphibolite Facies MB Mylonite	Infill foliation boudinage structures	Qtz±CC±Chl	0.5–4 cm	Toy et al. (2010)	Type iii
Foliation Parallel	AFZ	Below BDTZ (>6)	<1 km	Amphibolite Facies QFS & MB Mylonite	Parallel to mylonitic foliation	Qtz	0.5–2 cm	Toy et al. (2010)	Type i
IN Fissure	IN	Above BDTZ (<6)	5–10 km	Amphibolite & Greenschist Facies Schist	Open filling of large fractures	Qtz±CC±Chl ±Ad±Mus±Pyt	~10 cm	Craw (1988, 1997); Craw et al. (1994); Holm et al. (1989); Jenkin et al. (1994); Teagle et al. (1998)	Fissure veins
IN Ductile	IN	BDTZ (~6-8)	5–10 km	Amphibolite & Greenschist Facies Schist	Infill brittle-ductile faults and shears	Qtz±CC	0.5–2 cm	Holm et al. (1989); Wightman and Little (2007)	Syn-tectonic, Deformed veins, Boudinaged veins
MD Fissure	MD	Shallow (>3)	10–12 km	Greenschist and Sub-Greenschist Facies Schist	Infill fractures, joints and irregular cavities in wall rock	Qtz±CC±Ad ±Chl±Pyt	>10 cm	Craw (1997); Craw et al. (1987, 2009)	Type 3, Shallow
MD Au 1	MD	Above BDTZ (<6)	10–12 km	Greenschist and Sub-Greenschist Facies Schist	Infill steeply dipping fractures and shallowly dipping joints	Qtz±CC±Chl ±Ank±Pyt± Ars±Au±St	>10 cm	Craw (1997); Craw et al. (1987, 2009)	Type 1, Ankeritic
MD Au 2	MD	Above BDTZ (<6)	10–12 km	Greenschist and Sub-Greenschist Facies Schist	Infill fractures in steeply dipping fracture zones	Qtz±CC±Chl ±Biot±Mus±Ars ±Gal±Au	>10 cm	Craw (1997); Craw et al. (1987, 2009)	Type 2, Metamorphic

populations in vein quartz were characterised and subject to microthermometry. Quartz from ductilely deformed veins was investigated by Micro-Fourier Transform Infrared Spectroscopy (FT-IR). Hydrothermal mineral grains were removed from veins, sonicated in Milli-Q (18.2 MΩ.cm) water and purified by hand-picking.

Doubly polished ~250 μm thick slices were prepared from quartz veins for fluid inclusion observations and FT-IR analysis. Microthermometric measurements were performed on a Linkham THMS 600 heating stage at the University of Southampton following Hopkinson and Roberts (1996). Portions of the doubly polished wafers of ductilely deformed quartz veins were analysed using FT-IR to test for structurally bound hydrogen within quartz lattices following Gleeson et al. (2008).

Silicate $\delta^{18}O$ values were measured by laser fluorination following Sharp (1990) and δD values of fluid inclusions and hydrogen bearing minerals by *in vacuo* decrepitation following Donnelly et al. (2001) at the Scottish Universities Environmental Research Centre (see Supplementary Materials for details). Stable isotopes are reported using delta notation (Craig, 1961b) relative to V-SMOW. Full procedural reproducibility was $< 0.5‰$ for $\delta^{18}O$ values in natural samples. Reproducibility of δD values varies depending on sample type: $\pm 3‰$ for replicate analyses of NBS-30 (biotite), and $\pm 5‰$ for non-deformed and $\pm 10‰$ for deformed quartz fluid inclusion analyses.

3. Results

3.1. Fluid inclusions

Fluid inclusions (FI) in ductilely deformed veins from the AFZ are small (<12 μm), two (H_2O–CO_2) or three phase (H_2O–CO_2^v–CO_2^l) and are similar to those described in Toy et al. (2010). Secondary inclusions littered grain boundaries and there were numerous decrepitated inclusions, but those investigated were primary inclusions that showed no evidence of necking or fluid escape. On heating the vapour bubble shrank and homogenised to a supercritical fluid. The innermost bubbles (CO_2^v) in three phase inclusions homogenised with surrounding CO_2^l at temperatures between 28.6 and 32.4 °C. Foliation Boudinage veins have total homogenisation temperatures (T_h) of 243 to 380 °C with an average of 288 °C, although measurements are not normally distributed, with modes at ~290 and 330 °C (Fig. 2a). Excluding secondary inclusions, Foliation Parallel veins FI T_h range between 235 and 445 °C, with an average of 300 °C, and are also not normally distributed, with modes occurring at ~250 and 340 °C (Fig. 2a).

FZ Fissure veins have not been previously described and contain multi-faceted, three phase (H_2O–CO_2^v–CO_2^l) primary fluid inclusions up to 20 μm in size. T_h ranges from 241 to 428 °C with an average of 324 °C (Fig. 2b) and homogenisation of CO_2 occurs between 29.6 and 31.9 °C.

Inboard Fissure veins from Balfour Glacier (Craw et al., 1994) contain abundant large (up to 70 μm), well formed, rectangular primary FIs and smaller (<10 μm) secondary FIs along grain boundaries and fractures. Primary FIs have T_h lying within a narrow range from 245 to 272 °C with an average of 262 °C. These veins have lower T_h than Fissure veins from the Waiho and Fox Valleys north west of the area (Craw, 1988; Holm et al., 1989; Jenkin et al., 1994, Fig. 2b).

Main Divide veins contain small (<22 μm), equant, two phase FIs and secondary FIs occur along healed fractures. Primary FI T_h range from 209 to 328 °C with an average of 250 °C. These veins

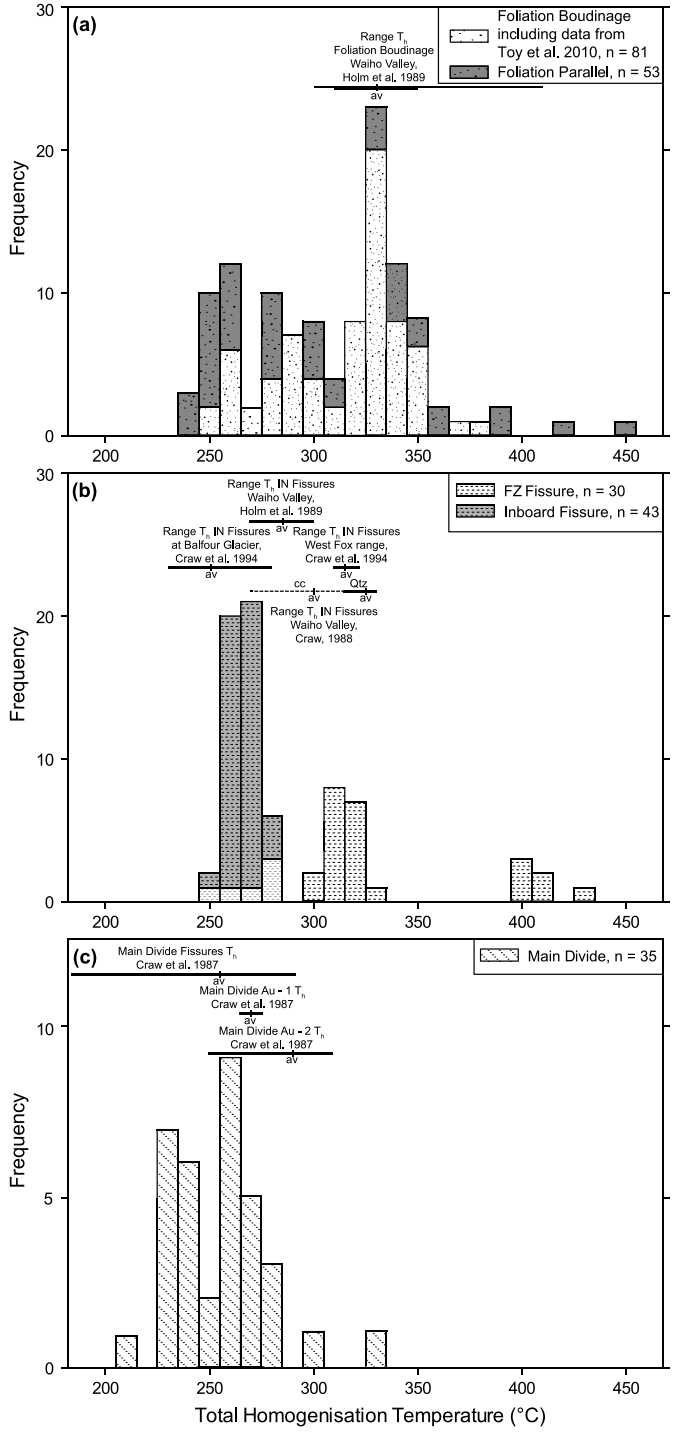

Fig. 2. Stacked histograms of quartz fluid inclusion total homogenisation temperatures (T_h). (a) Compilation of FI T_h of ductilely deformed veins from this study and Toy et al. (2010) compared with data from Holm et al. (1989). av = average T_h of published data. (b) Inboard and FZ Fissure vein FI T_h compared with data from Craw (1988), Craw et al. (1994), Holm et al. (1989). cc = calcite, Qtz = quartz. (c) Main Divide vein FI T_h data measured in this study compared with Craw et al. (1987).

have similar T_h as those recorded in previous studies (Craw et al., 1987, Fig. 2c). Due to being ~1 mm thick Joint Coating veins were not suitable for FI measurements.

3.2. FT-IR

During *in vacuo* thermal decrepitation of fluid inclusions for hydrogen isotope analyses, in some cases there is evidence that structurally bound hydroxyl complexes may be liberated in addition to molecular water, especially at higher temperatures (>1000 °C) (Gleeson et al., 2008). Li–OH and Al–OH species are commonly present in defects in deformed quartz. Although they may be present only in small quantities, Li and Al hydroxyl groups have very low δD values (−300 to −250‰, Gleeson et al., 2008) compared with included water. Consequently, even a small contribution from hydroxyl groups can produce δD values that are significantly lower than the isotopic signature of hydrothermal fluid captured in inclusions. To avoid contamination from hydroxyl groups we (1) checked for the presence of Al–OH and Li–OH in our samples by FT-IR and (2) during analyses samples were heated to only 700 °C.

Hydroxyl complexes, Al–OH and Li–OH appear as sharp absorption bands and shoulders due to OH stretching vibrations following the substitution of Si^{4+} by Al^{3+} (at 3385 and 3321 cm^{-1}) and Li^{+} (at 3485 and 3438 cm^{-1}) (Aines and Rossman, 1984; Grant et al., 2003; Kronenberg, 1994; Suzuki and Nakashima, 1999). FT-IR spectra were collected from all ductile vein samples and data is reported for ten samples that underwent fluid inclusion hydrogen isotope analysis. Other veins were not analysed for hydrogen isotopes due to insufficient sample, but the FT-IR spectra for these samples were similar to those reported in Table 2.

All samples showed broad absorption around 3400 cm^{-1} due to molecular water (Table 2, Aines and Rossman, 1984) with shoulders at around 3300 cm^{-1} indicating the presence of H^{+} in all samples except OU77948, a Foliation Parallel vein. Weak bands indicating the presence of minor Al–OH are present in all samples. In addition, samples EX1 and BWFB1 have weak bands between 3484 and 3486 cm^{-1} due to minor Li–OH (Fig. 3a). No samples display large Al–OH and Li–OH absorption peaks similar to those recorded by Grant et al. (2003) or Gleeson et al. (2008) (Fig. 3b).

Although only weakly defined, the presence of Al–OH and Li–OH groups means that liberation of structural hydrogen is possible during *in vacuo* thermal decrepitation of fluid inclusions. Previous studies have shown that heating of natural quartz to 1000 °C releases Li–OH molecules whereas Al–OH remain (Suzuki and Nakashima, 1999). BWFB1 and EX1 are the only samples that display the presence of Li–OH groups but also yield the lowest δD values (−111 and −98‰ respectively). This may be due to the release of structural hydrogen from Li–OH sites even with heating to only 700 °C, and hence we do not consider these analyses further. As all other ductile veins contain only Al–OH groups we consider analysed FI δD values are accurate measurements of the included hydrothermal fluids.

3.3. Stable isotopes

3.3.1. Oxygen isotopes

Oxygen isotopes of vein quartz show little variation other than from joint coatings, with $\delta^{18}O_{quartz} = 12.4 \pm 2.6$‰ ($2\sigma$, $n = 46$, Fig. 4a and Table S3). Vein quartz from Joint Coatings from the AFZ have much lower δ^{18}O values (2.5 and 2.6‰). Foliation Parallel and Foliation Boudinage ductile veins have quartz δ^{18}O average values of 11.5 and 13.1‰ respectively. The highest δ^{18}O values are in FZ and Inboard Fissure veins and Main Divide veins with averages of 13.2, 13.2 and 13.4‰ respectively. Chlorite was analysed from Foliation Parallel and Foliation Boudinage, Inboard Fissure and Main Divide veins, these data are similarly tightly grouped; δ^{18}O values are between 6.9 and 8.6‰, with no consistent variation between vein types (see Fig. 4b). One sample of adularia from an Inboard Fissure vein has a δ^{18}O value of 10.7‰.

3.3.2. D/H of fluid inclusions and chlorite

There is a wide range in accepted FI δD values from −84 to −45‰, with the lowest values from ductile veins and highest

Table 2
Outline of the shoulder and absorption band positions displayed in FT-IR spectra of each sample. Shoulders and absorption bands have been identified as specific point defects in quartz, specifically Al–OH and Li–OH groups. Shoulders below 2828 cm^{-1}, between 3345 and 3358 cm^{-1} and between 3360 and 3364 cm^{-1} do not have specific point defects attributed to their existence. np = not present.

Shoulder position (cm^{-1})										
Sample	HO	7.07.04	GH2	OU77948	BWFB3	OU81160	16.02.14	OU68307	EX1	BWFB1
Point defect										
?	3262	3206	3260	3209	3228	3223	np	3282	np	np
H^+	3303	3298	3300	np	3296	3300	3302	3303	3300	3303
?	np	np	3356	3357	3358	3347	3342	3348	3348	3345
?	np	np	np	np	np	3364	3360	np	np	3360
Al–OH	3382	3384	np	3376	3381	np	np	3379	3384	3379
Li^+	np	np	3394	np	np	3392	3393	3394	3392	3394
Li^+	np	np	np	np	np	np	3409	np	np	np
Al–OH	np	np	3425	3423	3426	3424	3426	np	3428	3425
Na^+	np	np	np	np	np	3454	np	np	np	3456
H^+	3469	3465	np	np	np	np	np	np	np	np
Li–OH	np	np	np	np	np	np	np	np	3484	3486
H^+, Na^+	3532	3534	np	np	np	3531	np	np	3531	3548
K^+, Na^+, Li^+	np	np	np	np	np	np	3562	3562	3550	3574
K^+	np	np	np	np	np	np	np	np	np	3608

from the Inboard Fissure and Main Divide veins (Figs. 3c and 5 and Table S4). Including the data from Jenkin et al. (1994) the range is −84 to −42‰ with an average of −58 ± 23‰ (2σ, $n = 27$), within range of local meteoric water (Fig. 6). Inboard Fissure veins have the highest yields (up to 0.15 μmol/mg) and highest δD values ranging from −73 to −46‰. Main Divide veins are similar but have slightly lower yields (0.04 to 0.09 μmol/mg) and a narrower range in δD values (−57 to −45‰) (Fig. 3c). Ductile veins range from −84 to −52‰ and have the lowest yields (0.006 to 0.05 μmol/mg). Yields of ductile veins are expected to be low because the fluid inclusions are small (<12 μm), some have been decrepitated, and much of the quartz has been dynamically recrystallised. Ductile veins have δD values within error of the range of non-deformed samples (−73 to −45‰, data summarised indirectly in Fig. 3c).

Chlorite δD values were also analysed and both chlorite and FI δD was analysed in some veins. In ductile veins there is a wide range in δD values of chlorite (−82 to −64‰, data summarised indirectly in Fig. 5), with two Foliation Boudinage veins having lower δD values (−72 and −82‰) than a Foliation Parallel vein (−64‰). FZ Fissure veins and Main Divide veins have a narrower range of chlorite δD values (−78 to −66‰).

4. Discussion

4.1. Estimation of stable isotope signatures of end-member fluids

Crustal fluids have distinctive isotopic ratios depending on fluid sources and flow paths that can be used to identify end-member fluids. As there is no syn-orogenic magmatic activity in the Southern Alps, end-member fluid compositions are restricted to meteoric waters and metamorphic dehydration fluids in equilibrium with Alpine Schist. In order to elucidate the Southern Alps fluid flow regimes we begin by estimating end-member fluid stable isotope signatures.

4.1.1. Meteoric fluids

Modern day isotopic compositions of meteoric waters are well constrained in the Southern Alps and rainwater lies on the global meteoric water line (GMWL, Craig, 1961a) with δD values ranging between −80 and −32‰ and δ^{18}O values between −11.2 and −5.5‰ (Stewart et al., 1983). Snow accumulating on the Franz Josef Glacier (to the West of the Main Divide) in the Southern Alps has δ^{18}O values from −23.3 to −9.4‰ and δD values from −177 to −58‰ (averages of −14.3 ± 3‰ and −102 ± 30‰ respectively, Purdie et al., 2010). These values provide lower limits of meteoric water signatures in the study area.

Fissure veins have been dated at ~800 ka (Teagle et al., 1998), and ductilely deformed veins that formed at ~6–8 km depth would take 600–800 ka to be exhumed at current uplift rates (up to 10 mm/yr, Norris and Cooper, 2007). The topography and orographic weather pattern of the Southern Alps should have been established within ~1 million years of the initiation of mountain building (Koons, 1989), and has changed little since the Pliocene (Cox and Sutherland, 2007; Craw et al., 2013). As seawater δ^{18}O values have varied by only ~1‰ over the last 700 ka (Lisiecki and Raymo, 2005), it is expected that stable isotope signatures of meteoric waters in the Southern Alps have not varied considerably over the time scales considered in this study. Therefore a reasonable range in isotopic compositions of the meteoric end-member fluid is −132 to −32‰ for δD and −17.3 to −5.5‰ for δ^{18}O values (Fig. 6).

Modelling meteoric water circulation: As meteoric waters percolate into the crust driven by the strong hydrological forces of the elevated Southern Alps topography, they will react with the host rocks. We have calculated water–rock reaction paths for fluids in equilibrium with Alpine Schist at different water–rock ratios and temperatures using Eq. (1) representing a closed system (Field and Fifarek, 1985, after Taylor, 1974, 1977) where the final composition of water (δ^f_w) after equilibrating with crustal rock (δ^i_r) depends on initial water isotopic composition (δ^i_w), the water–rock ratio (w/r = ratios of mass of O and H in water to rock) and temperature of water–rock interactions (which determines the water–rock fractionation factor, Δ_{r-w}).

$$\delta^f_w = \frac{\delta^i_r - \Delta_{r-w} + [(w/r)(\delta^i_w)]}{1 + (w/r)} \quad (1)$$

These paths have been modelled for both average rain (δ^{18}O = −8‰, δD = −54‰) and snow (δ^{18}O = −14‰, δD = −102‰) (Fig. 6b).

4.1.2. Calculation of fluid in equilibrium with Alpine Schist

Alpine Schist whole rock δ^{18}O values are taken from Cox (1993) and Vry et al. (2001) (ranging between 8 and 16‰) and whole rock mylonite and schist δD values from Vry et al. (2001) (ranging between −56 and −30‰), there is no apparent difference between δD values of Alpine Schist and mylonites. To estimate the composition of the potential metamorphic fluid end-member we have

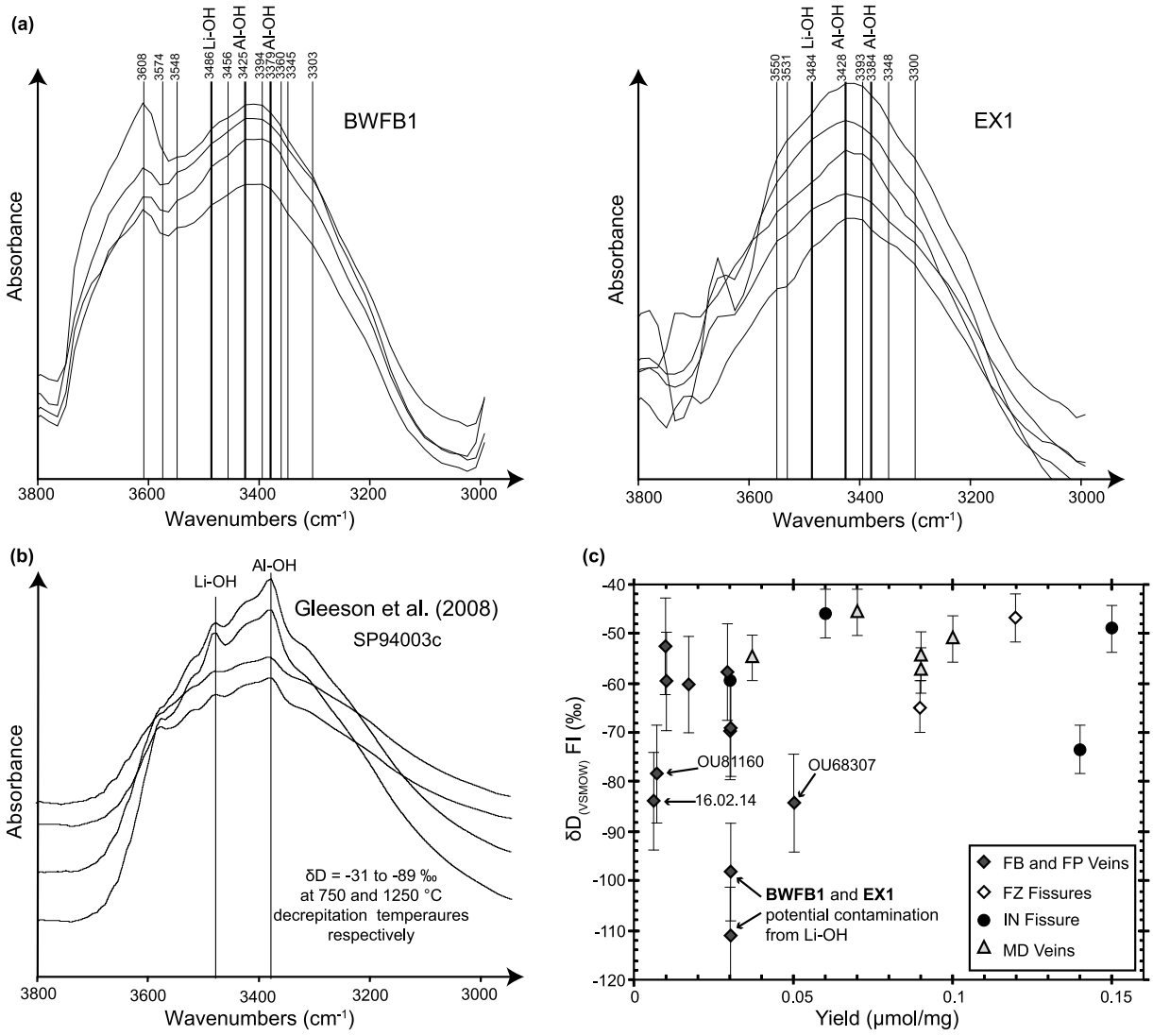

Fig. 3. (a) FT-IR absorbance spectra of Foliation Boudinage and Foliation Parallel quartz vein samples BWFB1 and EX1, showing minor absorption bands due to Al–OH and Li–OH as indicated. Vertical lines mark other shoulders present in these samples (see Table 2). The spectra are offset vertically for clarity. (b) FT-IR absorbance spectra of a cross course vein from Gleeson et al. (2008) showing large absorbance bands due to Al–OH and Li–OH. Note that absorbance bands are significantly more prominent than those measured in veins in this study. The sample had variable δD values depending on thermal decrepitation temperature. Higher temperature decrepitation (1250 versus 750 °C) resulted in δD values 58‰ lighter due to the release of hydrogen from Al–OH and Li–OH sites. (c) Yield versus fluid inclusion δD value. Foliation Parallel and Foliation Boudinage veins have the lowest yields and among the lowest δD values and Fissure veins have the highest yields and a large range in δD values. The two samples shown in (a) have lower δD values than other samples, possibly indicating contamination by the release of structural hydrogen from Li–OH sites. For this reason these samples have been discounted from the dataset. Three other ductile vein samples that have low δD values and yields are labelled. These samples do not display spectra indicative of Li–OH groups (see Table 2). FB = Foliation Boudinage veins; FP = Foliation Parallel veins; IN = Inboard.

calculated the isotopic composition of water in equilibrium with the metamorphic host rocks using measured whole rock isotopic compositions and modal percentages of minerals based on thin section observations of Alpine Schist. Fractionation factors between minerals and water were applied and fluid isotope ratios calculated weighted by the mass of oxygen or hydrogen in mineral structures and the proportions of minerals in the rock (Table 3). Changing the proportions of minerals in the end-member rocks does not significantly alter the calculated fluid compositions.

Metamorphic fluids released at higher temperatures produce fluids with lower δD and higher δ^{18}O values. Over the temperature range of 200 to 550 °C the estimated δ^{18}O values range between −0.5 and 17.5‰ and δD values range between −36 and +48‰, although such high positive numbers are unrealistic and are the result of extrapolating the fractionation equations for muscovite and biotite below their calibration limit of 400 °C. The predicted ranges of Southern Alps metamorphic fluid signatures is clearly different from New Zealand meteoric water (Fig. 6a).

4.2. Calculated fluid isotopic compositions from hydrothermal mineral data

The δ^{18}O composition of vein-forming fluids have been estimated using mineral analyses, mineral specific fractionation equations (Matsuhisa et al. (1979) for quartz, Cole and Ripley (1999) for chlorite and O'Neil and Taylor (1967) for adularia, see Table 3 and Supplementary Materials), and temperature estimates from fluid inclusion microthermometry. Calculated fluid δ^{18}O values in all vein types (excluding Joint Coatings) have a similar tight grouping as $\delta^{18}O_{quartz}$ values, albeit with a wider range (2.3 to 8.7‰, average 5.4‰, $n = 55$). These vein-forming fluids are within the estimated range of rock-equilibrated/metamorphic waters (Fig. 4b). Joint Coating veins have δ^{18}O fluid values similar to meteoric water.

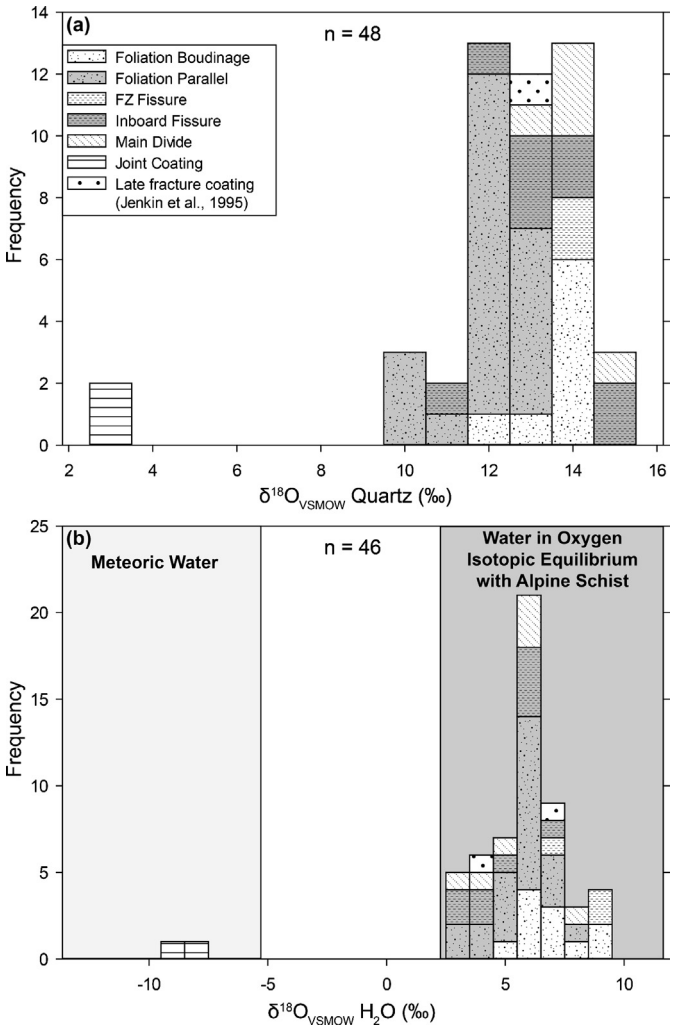

Fig. 4. Stacked histograms showing (a) the range in measured $\delta^{18}O$ values of quartz and (b) the calculated $\delta^{18}O$ values of water in equilibrium with quartz and other vein minerals (chlorite and adularia). Water $\delta^{18}O$ values were calculated as described in the main text using fluid inclusion temperatures (see Table S3 in the Supplementary Materials). In (b) the boxes are estimates of $\delta^{18}O$ values of end member fluids: fluids in equilibrium with Alpine Schist and meteoric waters. Data from Jenkin et al. (1994) are included.

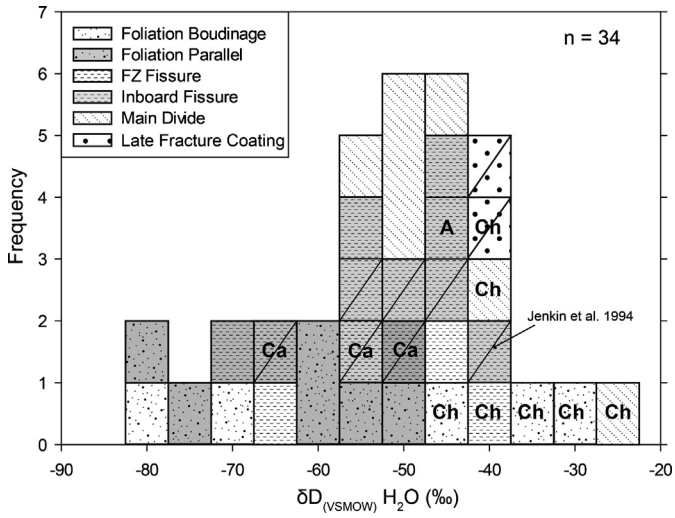

Fig. 5. Stacked histogram of fluid inclusion δD values from quartz veins from different structural levels in the Southern Alps. Additional data include a single adularia (A) analysis from an Inboard Fissure vein and quartz and calcite (C) data from Jenkin et al. (1994) (diagonal stroke). δD composition of water in equilibrium with chlorite (Ch) is calculated as outlined in the main text following Graham et al. (1984, 1987).

Textures in all vein types indicate that chlorite formation postdated quartz precipitation and hence fluid compositions and/or temperatures may have changed. Fluid in equilibrium with chlorite (using Graham et al., 1984, 1987) has δD values ranging between −49 and −29‰, up to ∼10‰ higher than FI δD values from the same vein generations (Fig. 5). Chlorite from a "late fracture coating" also falls within this range (δD_{H_2O} = −44 to −38‰, for temperatures of 200 to 320 °C, Jenkin et al., 1994). Chlorite from a FZ Fissure vein (NG8) indicates equilibrium with a fluid with δD_{H_2O} value of −44‰ (at the average FI homogenisation temperature, 290 °C) within error of the FI δD_{quartz} values −47‰. In contrast, chlorites in Main Divide veins (Burton 1e and Callery 1) suggest δD_{H_2O} values that are ∼16‰ higher than FI δD values at the measured fluid inclusion temperatures. Similarly chlorite from Foliation Boudinage veins (ZF4, NBLS1 and HA) indicate formation from fluids with δD_{H_2O} values between −49 and −31‰. These chlorite-derived δD_{H_2O} values are higher than Foliation Boudinage FI δD values (−84 to −70‰). These differences may arise because the veins were precipitated from fluids with different stable isotope signatures, at different temperatures or due to the extrapolation of the chlorite-water hydrogen fractionation equation to temperatures below the calibration range (<500 °C, Graham et al., 1987).

4.3. The balance between meteoric water circulation and metamorphic dewatering

4.3.1. Fluid sources: meteoric versus metamorphic waters

At levels deeper than Joint Coating veins (∼2 km depth) vein-forming fluids have consistently high $\delta^{18}O$ values (2.3 to 8.7‰). All estimated vein-forming fluids are rock-exchanged with $\delta^{18}O$ and δD values lying on or between the 250 to 450 °C water–rock reaction lines at low water–rock ratios (between 0.01 to 0.1, Fig. 6b).

Our data show that none of the estimated fluids are purely metamorphic in origin. However, all vein compositions can be explained as forming from evolved meteoric fluids that have isotopically exchanged with Alpine Schists. Variability in $\delta^{18}O$ values between samples is likely due to fluid–rock interaction along different fluid flow paths, as host rock $\delta^{18}O$ values are variable, ranging between 8 and 16‰ (Cox, 1993; Vry et al., 2001). Although there remains the possibility that the signatures observed could be produced by the mixing of meteoric and metamorphic fluids, in such a scenario, the deeper, ductilely-deformed veins should have proportionally higher metamorphic fluid component and therefore higher δD values than the shallower-formed veins; the opposite to what is measured (Fig. 6b and Table S4). This strongly indicates that metamorphic fluids are not substantially present and that meteoric fluids precipitated the vein minerals that formed in the ductile regime.

The variation in δD values between and within vein sets can be attributed to initial differences in meteoric δD values at differing altitudes. In the Inboard zone of the Southern Alps, topography grows from ∼300 m adjacent to the Alpine Fault to >3000 m 15 km east at the Main Divide. This range in relief has a large effect on surface water δD values across the area (−132 to −32‰, Purdie et al., 2010; Stewart et al., 1983) and therefore on the range of δD values of meteoric fluids percolating into the crust. The low δD values of ductile vein-forming fluids indicates that they were dominantly derived from high altitude or snow-derived meteoric waters.

4.3.2. Estimated end member fluid fluxes

The following is an order-of-magnitude estimation of the quantities of meteoric water compared with that produced by metamorphism. A crustal root has been imaged beneath the Southern Alps from gravity and seismic data which is ∼50 km perpendicular

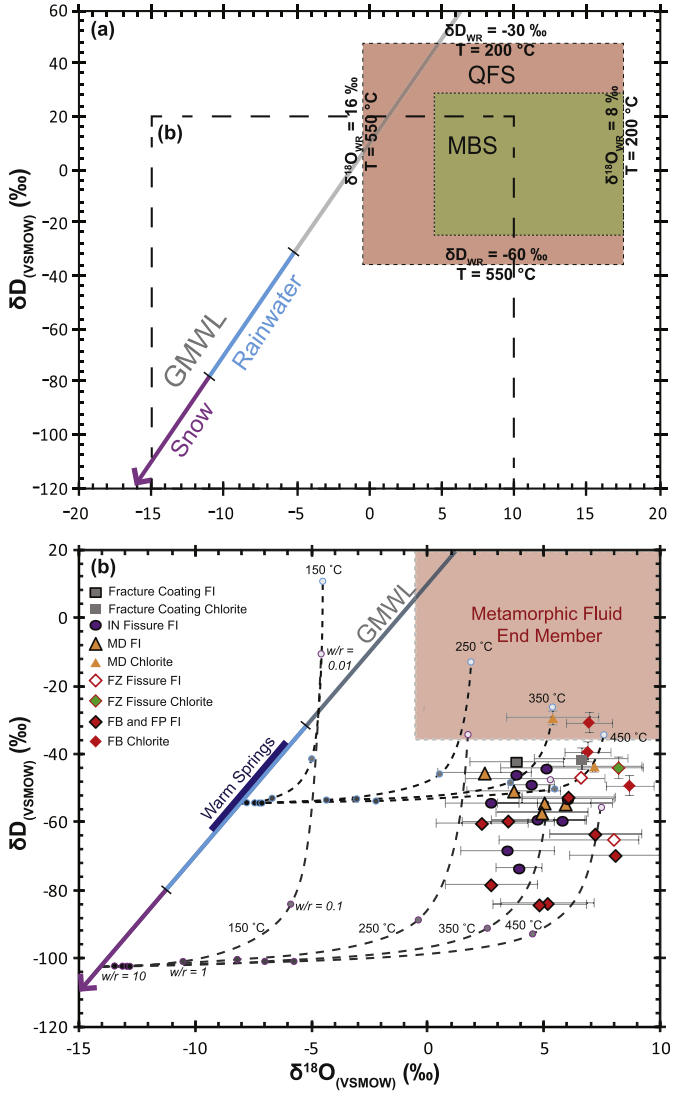

Fig. 6. (a) Range of δD and δ^{18}O values of water in equilibrium with quartzofeldspathic (QFS) and metabasic (MBS) Alpine Schist calculated as described in the main text. Global Meteoric Water Line (GMWL) of Craig (1961a) and range of rainwater and snow for South Island and the Southern Alps following Stewart et al. (1983) and Purdie et al. (2010). $\delta^{18}O_{WR}$ and δD_{WR} are whole rock isotopic values used to calculate metamorphic fluid compositions. Area within dashed line is shown in (b). (b) Calculated δ^{18}O of water in equilibrium with the vein minerals, based on fluid inclusion total homogenisation temperatures, versus measured FI δD and calculated δD of water in equilibrium with chlorite (including data from Jenkin et al. (1994)). Modelled closed system water–rock isotopic exchange pathways calculated using Eq. (1) (dashed arcs). Stable isotope values of local warm spring waters from Barnes et al. (1978); Reyes et al. (2010). Error bars for δ^{18}O values of quartz and δ^{18}O and δD values of chlorite represent the range in possible temperatures of formation of the veins based on ranges of fluid inclusion homogenisation temperatures. MD = Main Divide; FB = Foliation Boudinage; FP = Foliation Parallel; IN = Inboard Fissure.

to the plate boundary and 5–10 km thick (Davey et al., 2007; Herman et al., 2009; Stern et al., 2007) and this zone is where present-day metamorphism is likely to be occurring. The potential metamorphic fluid flux can be estimated using the volume of water liberated during greenschist facies to amphibolite facies prograde metamorphism occurring within the core of the orogen. These dehydration reactions yield ~1 wt.% water (Pitcairn et al., 2006), equivalent to 0.028 km^3 of water per 1 km^3 of rock passing through the orogen. To estimate metamorphic fluid production we consider a length of 50 km along the orogen and the present day convergent component of plate motion ($\sim 10^{-2}$ m/yr, Norris and Cooper, 2007). A 5–10 km thick rock packet will move through this 50 km wide zone in ~5 Myr and become metamorphosed to amphibolite facies. Dehydration reactions will liberate 3.5×10^{11} to 7×10^{11} m^3 of water, equivalent to 7×10^4 to 1.4×10^5 m^3/yr production from this zone. However, it is likely that much of this fluid will be trapped on grain boundaries and only released during uplift (Norris and Henley, 1976; Wannamaker et al., 2002).

In contrast, the western slopes of the Southern Alps receive exceptionally high precipitation, up to 12 m/yr rainfall (Woods et al., 2006). Average rainfall over the investigated 50×50 km^2 area is ~6.4 m/yr, which equates to 10^{10} m^3/yr of rain. Assuming the infiltration proportion is between 0.1 and 10%, meteoric water inputs are estimated at between 10^7 to 10^9 m^3/yr, at least two orders of magnitude higher than estimated metamorphic water production. In order for metamorphic waters to be detectable by stable isotopes above the BDTZ where meteoric waters dominate, the plate convergence rate would need to be at least an order of magnitude higher (>100 mm/yr), even then the maximum yearly metamorphic water production would be at most ~5% of the most conservative estimate of the meteoric water flux (on the order 10^6 m^3/yr). Alternatively, runoff and evapotranspiration would need to be an unusually large proportion of the total rainfall with infiltration <0.001% for the metamorphic fluid production to be of a similar magnitude. Hence in an active orogen with high topography and precipitation it is to be expected that hydrothermal fluid flow in the brittle crust is greatly dominated by meteoric waters, in agreement with stable isotope analyses from this and previous studies (Horton et al., 2003; Jenkin et al., 1994).

4.4. Penetration of surface-derived fluids into the ductile regime

The penetration of surface-derived fluids into the ductile regime remains conceptually challenging. However, light hydrogen isotope signatures (δD values of −84 to −52‰) liberated from fluid inclusions within ductilely deformed quartz veins hosted by mylonites in the AFZ require the penetration of meteoric fluids into the base of the BDTZ. These stable isotopic signatures can be achieved solely by evolved meteoric fluids, or mixing between a less evolved meteoric fluid and a minor proportion of metamorphic water. Either way a major proportion of meteoric water is required.

The incursion of meteoric fluids into the ductile portion of the crust has been suggested in previous studies (e.g. Barker et al., 2000; Clark et al., 2006; Fricke et al., 1992; McCaig et al., 1990; Raimondo et al., 2011; Upton et al., 1995), but compelling evidence has remained elusive. Most studies (e.g. Barker et al., 2000; Clark et al., 2006; Fricke et al., 1992; McCaig et al., 1990; Raimondo et al., 2011) were carried out in exhumed ancient collision zones where the tectonics are not well constrained or magmatic waters may have circulated. Other studies (e.g. Upton et al., 1995) use only δ^{18}O values as evidence for penetration of meteoric waters, but as shown earlier oxygen isotopes do not provide a unambiguous tracer of metamorphic fluid. Low δD values have been liberated from fluid inclusions hosted in deep crustal shear zones (Barker et al., 2000), but these quartz samples were not checked for the presence of structural hydroxyl groups (Al–OH and Li–OH) that could be the source of light hydrogen.

Some studies of ancient collision zones (Clark et al., 2006; Raimondo et al., 2013) explain the meteoric-like signatures in ductile rocks as the product of shallow level alteration prior to burial and subsequent ductile deformation or near surface alteration of host rocks prior to reburial and devolatisation producing metamorphic waters with meteoric-like isotopic signatures. However, in the Southern Alps primary fluid inclusions with meteoric δD values are preserved within veins that post-date the onset of

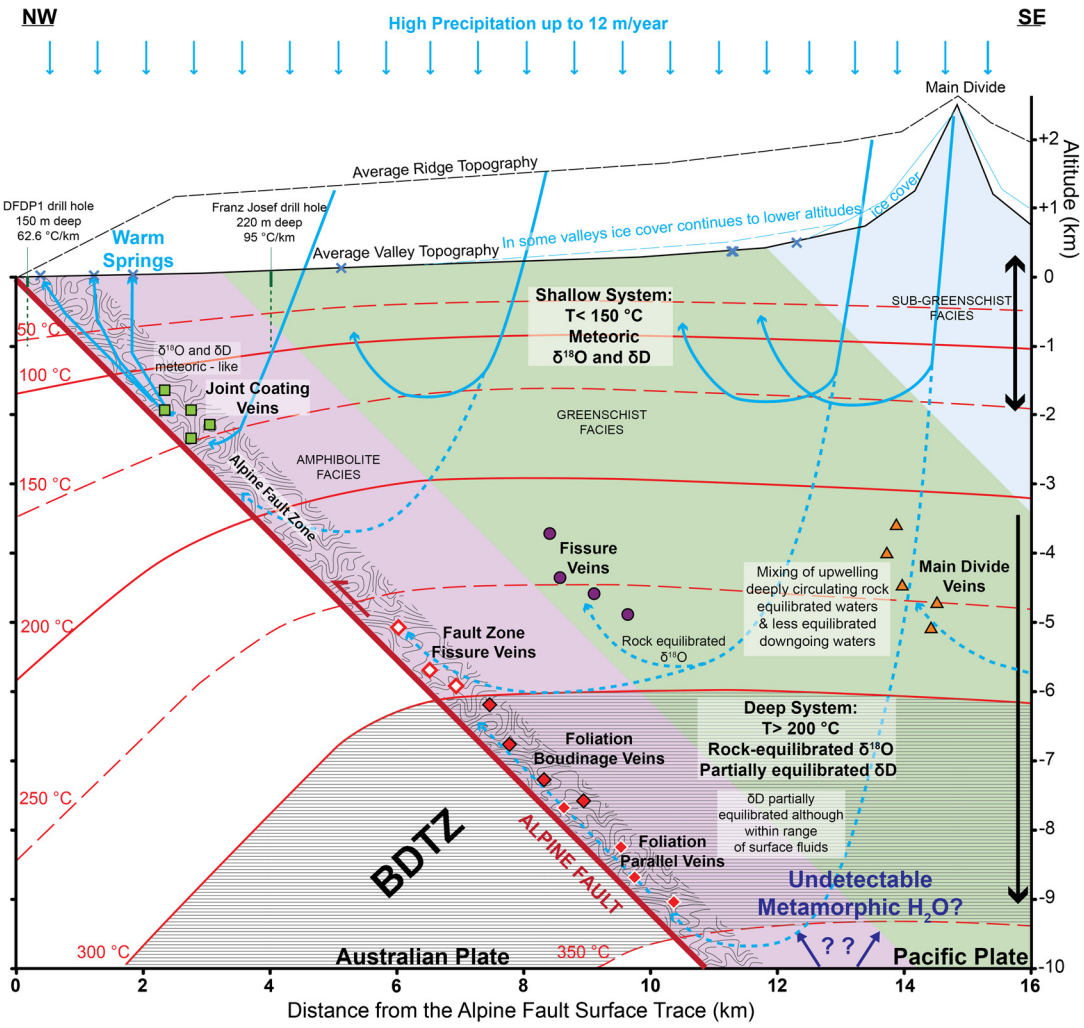

Fig. 7. Summary schematic of the fluid flow regime in the Southern Alps. Estimated isotherms adapted from Toy et al. (2010) and Craw (1997). Vein formation depths are based on measurements and the temperature profile presented. Geothermal gradients measured in the DFDP1 and Franz Josef drillholes are from Sutherland et al. (2012) and Shi et al. (1996) respectively.

Table 3
Table shows the mineral percentages estimated for quartzofeldspathic schist (QFS) and metabasic schist (MBS), the percentage of each mineral that is made up by hydrogen (H) and oxygen (O) and the fractionation factors applied to each mineral for hydrogen and oxygen. References are as follows: 1 – Matsuhisa et al. (1979), 2 – Zheng (1993b), 3 – Suzuoki and Epstein (1976), 4 – O'Neil and Taylor (1969), 5 – Zheng (1993a), 6 – Wenner and Taylor (1971), 7 – Graham et al. (1984), 8 – Graham et al. (1980), 9 – Chacko et al. (1999).

Mineral	Proportion		% in mineral		$1000 \ln \alpha$		Ref.
	QFS	MBS	H	O	Hydrogen	Oxygen	
Quartz	53%	5%	0	53.3	–	$3.34(\frac{10^6}{T^2}) - 3.31$	1
Biotite	15%	5%	0.46	43.4	$-21.3(\frac{10^6}{T^2}) - 2.8$	$3.84(\frac{10^6}{T^2}) - 8.87(\frac{10^3}{T}) + 2.46$	2,3
Muscovite	15%	0%	0.50	47.4	$-22.1(\frac{10^6}{T^2}) + 19.1$	$2.38(\frac{10^6}{T^2}) - 3.89$	4,3
Albite	5%	10%	0	48.7	–	$4.33(\frac{10^6}{T^2}) - 6.15(\frac{10^3}{T}) + 1.98$	5
Anorthite	5%	10%	0	46.1	–	$4.12(\frac{10^6}{T^2}) - 7.5(\frac{10^3}{T}) + 2.24$	5
Chlorite	3%	15%	1.34	48.4	$-3.7(\frac{10^6}{T^2}) - 24$	$1.56(\frac{10^6}{T^2}) - 4.7$	6,7
Garnet	1.5%	5%	0	42.6	–	$3.74(\frac{10^6}{T^2}) - 9.11(\frac{10^3}{T}) + 2.52$	5
Epidote	0.5%	10%	0.19	40.1	$29.2(\frac{10^6}{T^2}) - 138.8$	$4.05(\frac{10^6}{T^2}) - 7.81(\frac{10^3}{T}) + 2.29$	2,8,9
Titanite	0.5%	5%	0	40.5	–	$3.81(\frac{10^6}{T^2}) - 8.87(\frac{10^3}{T}) + 2.49$	5
Horneblende	1.5%	35%	0.24	46.8	$-23.9(\frac{10^6}{T^2}) + 7.9$	$3.89(\frac{10^6}{T^2}) - 8.56(\frac{10^3}{T}) + 2.43$	2,3

mylonitisation and are then further ductilely deformed, precluding the possibility that the signature formed within shallow veins before burial within the orogen. As the rocks hosting the ductilely deformed veins were at 25–30 km depth prior to the onset of late Tertiary exhumation (Cooper, 1980; Cox and Sutherland, 2007; Norris and Cooper, 2007), and the absence of meteoric isotopic signatures in mylonitic host rocks, we discount the possibility that the host rocks were altered in the near surface prior to reburial (cf. Raimondo et al., 2013).

Theoretical models indicate that the penetration of meteoric waters into the ductile regime of an orogen is mechanically possible. Active deformation within the ductile regime of orogenic

belts can create local dilations, particularly where different rock types are present, which allow fluid movement against widely assumed regional hydraulic gradients (McCaig, 1988; Sibson, 1981, 1992a; Upton et al., 1995). Alternatively, the vertical position of the BDTZ may change during seismic cycles allowing fluids to penetrate deeply under hydrostatic pressure before becoming overprinted by ductile deformation as the BDTZ returns to higher levels (Connolly and Podladchikov, 2004; Sibson, 1992b; Wightman and Little, 2007). Such models only allow for the migration of small fluid volumes, and the relatively long stagnation periods between pumping events increases the probability of rock-buffering, in agreement with our rock-buffered fluid $\delta^{18}O$ values.

4.5. A model of fluid flow in the Southern Alps

Stable isotope analysis of vein minerals and fluid inclusions indicates the hydrothermal systems beneath the Southern Alps are dominated by meteoric water to depths of at least 6 to 8 km. In the upper ~2 km of the crust the hydrothermal fluids responsible for precipitation of Joint Coating veins and that emanate in warm springs have meteoric-like $\delta^{18}O$ and δD values due to only limited water–rock exchange at low temperatures (<150 °C, Reyes et al., 2010) (Fig. 7). There is a greater degree of fluid–rock equilibration at increasing depths and temperatures leading to meteoric fluids with evolved $\delta^{18}O$ values that are indistinguishable from metamorphic fluids. In such instances more enduring tracers of fluid flow, such as hydrogen isotopes, are essential to unambiguously identify fluid sources. Here we show evolved meteoric waters are the principal mineralising fluids at all crustal levels down to and in to the ductile regime. This does not preclude the presence of a metamorphic component but it must be too small in the brittle regime to be detected by hydrogen isotopes and only minor in the BDTZ and below.

5. Conclusions

1. Fluids circulating at <2 km depth have meteoric $\delta^{18}O$ and δD values indicating the fluids are meteoric and have undergone only limited oxygen and hydrogen isotopic exchange with host rocks. Oxygen isotopes of vein-forming fluids at deeper levels are indistinguishable from calculated metamorphic fluid signatures, but δD values of fluid inclusions in these minerals identifies them as originally meteoric waters that have equilibrated oxygen with host rocks.
2. A conservative estimate of meteoric water infiltration indicates that the meteoric water flux above the brittle to ductile transition zone is at least two orders of magnitude greater than the potential metamorphic water production from below. No minerals analysed from fractures within the brittle crust require the presence of metamorphic water, therefore the fluid circulating to ~6 depth in the Southern Alps is dominantly surface-derived.
3. Ductilely deformed veins that post-date the onset of Alpine Fault zone mylonitisation and are further ductilely deformed, preserve primary fluid inclusions that show no evidence for the presence of structural hydrogen. Low δD values of included waters require the penetration of meteoric fluids into the ductile regime of the orogen. The stable isotopic signatures of the mineralising fluids can be achieved solely by evolved meteoric fluids, or mixing a less evolved meteoric fluid with a minor proportion of metamorphic water. Either way the ductilely deformed quartz veins that preserve the fluid inclusions were formed from waters that were dominantly meteoric in origin.

Acknowledgements

We gratefully acknowledge Virginia Toy for provision of samples and advice on microstructural analysis, Nick Goodwin for provision of samples, and James Nowecki and Ross Williams for training and advice on fluid inclusion and FT-IR analyses, Bob Jones and John Ford for preparing thin sections and fluid inclusion wafers, and Alison MacDonald for help with stable isotope analyses. C.D.M. acknowledges Natural Environment Research Council – CASE PhD studentship award NE/G524160/1 (GNS Science CASE partner). D.A.H.T. acknowledges NERC grants NE/H012842/1 and NE/J024449/1, and a Royal Society Wolfson Research Merit Award (WM130051) that have supported this research. A.J.B. is funded by NERC Isotope Community Support Facility at the Scottish Universities Environmental Research Centre and stable isotope analyses and training for this project were funded through the award of a NERC Facilities grant to D.A.H.T. and C.D.M. (IP/1187/0510). We gratefully acknowledge comments from Alex Webber, editorial advice and comments from Tim Elliott, and reviews from Tom Raimondo and an anonymous reviewer that improved this manuscript.

Appendix A. Supplementary material

Supplementary material related to this article can be found online at http://dx.doi.org/10.1016/j.epsl.2014.04.046.

References

Aines, R.D., Rossman, G.R., 1984. Water in minerals – a peak in the infrared. J. Geophys. Res. 89, 4059–4071.
Barker, A.J., Bennett, D.G., Boyce, A.J., Fallick, A.E., 2000. Retrogression by deep infiltration of meteoric fluids into thrust zones during late-orogenic rapid unroofing. J. Metamorph. Geol. 18, 307–318.
Barnes, I., Downes, C.J., Hurlston, J.R., 1978. Warm Springs, South Island New Zealand and their potentials to yield Laumontite. Am. J. Sci. 278, 1412–1427.
Bickle, M.J., McKenzie, D., 1987. The transport of heat and matter by fluids during metamorphism. Contrib. Mineral. Petrol. 95, 384–392.
Burrows, D.R., Wood, P.C., Spooner, E.T.C., 1986. Carbon isotope evidence for a magmatic origin for Archaean gold–quartz vein ore deposits. Nature 321, 851–854.
Chacko, T., Riciputi, L.R., Cole, D.R., Horita, J., 1999. A new technique for determining equilibrium hydrogen isotope fractionation factors using the ion microprobe: application to the epidote–water system. Geochim. Cosmochim. Acta 63, 1–10.
Chamberlain, C.P., Zeitler, P.K., Barnett, D.E., Winslow, D., Poulson, S.R., Leahy, T., Hammer, J.E., 1995. Active hydrothermal systems during the recent uplift of Nanga Parbat, Pakistan Himalaya. J. Geophys. Res., Solid Earth 100, 439–453.
Clark, C., Hand, M., Faure, K., Mumm, A.S., 2006. Up-temperature flow of surface-derived fluids in the mid-crust: the role of pre-orogenic burial of hydrated fault rocks. J. Metamorph. Geol. 24, 367–387.
Cole, D.R., Ripley, E.M., 1999. Oxygen isotope fractionation between chlorite and water from 170 to 350 °C: a preliminary assessment based on partial exchange and fluid/rock experiments. Geochim. Cosmochim. Acta 63, 449–457.
Connolly, J.A.D., Podladchikov, Y.Y., 2004. Fluid flow in compressive tectonic settings: implications for midcrustal seismic reflectors and downward fluid migration. J. Geophys. Res. 109, B04201.
Cooper, A.F., 1980. Retrograde alteration of chromian kyanite in metachert and amphibolite whiteschist from the Southern Alps, New Zealand, with implications for uplift on the Alpine Fault. Contrib. Mineral. Petrol. 75, 153–164.
Cox, S.C., 1993. Veins, fluid, fractals, scale and schist. Ph.D. thesis. University of Otago.
Cox, S.C., Barrell, D.J.A., 2007. Geology of the Aoraki area. Institute of Geological and Nuclear Sciences 1:250 000 geological map 15. 1 sheet + 71 p. Lower Hutt, New Zealand. GNS Science.
Cox, S.C., Sutherland, R., 2007. Regional geological framework of South Island, New Zealand, and its significance for understanding the Active Plate Boundary. In: Okaya, D., Stern, T., Davey, F. (Eds.), Continent–Continent Collision at the Pacific/Indo Australian Plate Boundary: Background, Motivation and Principal Results. In: Geophysical Monograph, vol. 175. American Geolphysical Union, Washington, DC, pp. 19–46.
Craig, H., 1961a. Isotopic variations in meteoric waters. Science 133, 1702–1703.
Craig, H., 1961b. Standard for reporting concentrations of deuterium and oxygen-18 in natural waters. Science 133, 1833–1834.
Craw, D., 1988. Shallow-level metamorphic fluids in a high uplift rate metamorphic belt, Alpine Schist, New Zealand. J. Metamorph. Geol. 6, 1–16.
Craw, D., 1997. Fluid inclusion evidence for geothermal structure beneath the Southern Alps, New Zealand. N.Z. J. Geol. Geophys. 40, 43–52.

Craw, D., Campbell, J.R., 2004. Tectonic and structural setting for active mesothermal gold vein systems, Southern Alps, New Zealand. J. Struct. Geol. 26, 995–1005.
Craw, D., Druzbicka, J., Rufaut, C., Waters, J., 2013. Geological controls on palaeo-environmental change in a tectonic rain shadow, Southern New Zealand. Palaeogeogr. Palaeoclimatol. Palaeoecol. 370, 103–116.
Craw, D., Rattenbury, M.S., Johnston, R.D., 1987. Structural geology and vein mineralisation in the Callery River headwaters, Southern Alps, New Zealand. N.Z. J. Geol. Geophys. 30, 273–286.
Craw, D., Rattenbury, M.S., Johnstone, R.D., 1994. Structures within greenschist facies Alpine Schist, central Southern Alps, New Zealand. N.Z. J. Geol. Geophys. 37, 101–111.
Craw, D., Upton, P., MacKenzie, D.J., 2009. Hydrothermal alteration styles in ancient and modern orogenic gold deposits, New Zealand. N.Z. J. Geol. Geophys. 52, 11–26.
Davey, F., Eberhart-Phillips, D., Kohler, M.D., Bannister, S., Caldwell, G., Henrys, S., Scherwath, M., Stern, T., Van Avendonk, H.J.A., 2007. Geophysical Structure of the Southern Alps Orogen, South Island, New Zealand. Geophysical Monograph, vol. 175. American Geophysical Union, Washington DC, pp. 47–73.
DeMets, C., Gordon, R.G., Argus, D.F., 2010. Geologically current plate motions. Geophys. J. Int. 181, 1–80.
Donnelly, T., Waldron, S., Tait, A., Dougans, J., Bearhop, S., 2001. Hydrogen isotope analysis of natural abundance and deuterium-enriched waters by reduction over chromium on-line to a dynamic dual inlet isotope-ratio mass spectrometer. Rapid Commun. Mass Spectrom. 15, 1297–1303.
Field, C.W., Fifarek, R.H., 1985. Light Stable-Isotope Systematics in the Epithermal Environment. Rev. Econ. Geol., vol. 2. Society of Economic Geologists, pp. 99–128. Chapter 6.
Fricke, H.C., Wickham, S.M., O'Neil, J.R., 1992. Oxygen and hydrogen isotope evidence for meteoric water infiltration during mylonitization and uplift in the Ruby Mountains–East Humboldt Range core complex, Nevada. Contrib. Mineral. Petrol. 111, 203–221.
Fusseis, F., Regenauer-Lieb, K., Liu, J., Hough, R.M., Carlo, F.D., 2009. Creep cavitation can establish a dynamic granular fluid pump in ductile shear zones. Nature 459, 974–977.
Gleeson, S.A., Roberts, S., Fallick, A.E., Boyce, A.J., 2008. Micro-Fourier Transform Infrared (FT-IR) and δD value investigation of hydrothermal vein quartz: interpretation of fluid inclusion δD values in hydrothermal systems. Geochim. Cosmochim. Acta 72, 4595–4606.
Graham, C.M., Atkinson, J., Harmon, R.S., 1984. Hydrogen isotope fractionation in the system chlorite–water. Prog. Exp. Petrol. 6, 139–140.
Graham, C.M., Sheppard, S.M.F., Heaton, T.H.E., 1980. Experimental hydrogen isotope fractionation factors in the system epidote–H_2O, zoisite–H_2O and AlO(OH)–H_2O. Geochim. Cosmochim. Acta 44, 353–364.
Graham, C.M., Viglino, J.A., Harmon, R.S., 1987. Experimental study of hydrogen-isotope exchange between aluminous chlorite and water and of hydrogen diffusion in chlorite. Am. Mineral. 72, 566–579.
Grant, K., Gleeson, S.A., Roberts, S., 2003. The high-temperature behavior of defect hydrogen species in quartz: implications for hydrogen isotope studies. Am. Mineral. 88, 262–270.
Groves, D.I., 1993. The crustal continuum model for late-archaean lode-gold deposits of the Yilgarn block, Western Australia. Miner. Depos. 28, 366–374.
Herman, F., Cox, S.C., Kamp, P.J.J., 2009. Low-temperature thermochronology and thermokinematic modeling of deformation, exhumation, and development of topography in the central Southern Alps, New Zealand. Tectonics 28.
Holm, D.K., Norris, R.J., Craw, D., 1989. Brittle and Ductile deformation in a zone of rapid uplift: central Southern Alps, New Zealand. Tectonics 8, 153–168.
Hopkinson, L., Roberts, S., 1996. Fluid evolution during tectonic exhumation of oceanic crust at a slow-spreading paleoridge axis: evidence from the Lizard ophiolite UK. Earth Planet. Sci. Lett. 141, 125–136.
Horton, T.W., Blum, J.D., Craw, D., Koons, P.O., Chamberlain, C.P., 2003. Oxygen, carbon, and strontium isotopic constraints on timing and sources of crustal fluids in an active orogen: South Island, New Zealand. N.Z. J. Geol. Geophys. 46, 457–471.
Jenkin, G.R.T., Craw, D., Fallick, A.E., 1994. Stable isotopic and fluid inclusion evidence for meteoric fluid penetration into an active mountain belt: Alpine Schist, New Zealand. J. Metamorph. Geol. 12, 429–444.
Kennedy, B.M., van Soest, M.C., 2007. Flow of mantle fluids through the ductile lower crust: helium isotope trends. Science 318, 1433–1436.
Koons, P.O., 1987. Some thermal and mechanical consequences of rapid uplift: an example from the Southern Alps, New Zealand. Earth Planet. Sci. Lett. 89, 307–319.
Koons, P.O., 1989. The topographic evolution of collisional mountain belts: a numerical look at the Southern Alps, New Zealand. Am. J. Sci. 289, 1041–1069.
Koons, P.O., Craw, D., 1991. Evolution of fluid driving forces and composition within collisional orogens. Geophys. Res. Lett. 18, 935–938.
Koons, P.O., Craw, D., Cox, S.C., Upton, P., Templeton, A.S., Chamberlain, C.P., 1998. Fluid flow during active oblique convergence: a Southern Alps model from mechanical and geochemical observations. Geology 26, 159–162.
Kronenberg, A.K., 1994. Hydrogen speciation and chemical weakening in quartz. Rev. Mineral. Geochem. 29, 123–176.
Leitner, B., Eberhart-Phillips, D., Anderson, H., Nabelek, J., 2001. A focused look at the Alpine fault, New Zealand: seismicity, focal mechanisms, and stress observations. J. Geophys. Res. 102, 2193–2220.
Lisiecki, L.E., Raymo, M.E., 2005. A Pliocene–Pleistocene stack of 57 globally distributed benthic δ^{18}O records. Paleoceanography 20, PA1003.
Matsuhisa, Y., Goldsmith, J.R., Clayton, R.N., 1979. Oxygen isotopic fractionation in the system quartz–albite–anorthite–water. Geochim. Cosmochim. Acta 43, 1131–1140.
McCaig, A.M., 1988. Deep fluid circulation in fault zones. Geology 16, 867–870.
McCaig, A.M., Wickham, S.M., Taylor, H.P., 1990. Deep fluid circulation in Alpine Shear zones, Pyrenees, France – field and oxygen isotope studies. Contrib. Mineral. Petrol. 106, 41–60.
Norris, R.J., Cooper, A.F., 2007. The Alpine Fault, New Zealand: surface geology and field relations. In: Okaya, D., Stern, T., Davey, F. (Eds.), A Continental Plate Boundary: Tectonics at South Island, New Zealand. In: Geophysical Monograph, vol. 175. American Geophysical Union, Washington, DC, pp. 157–175.
Norris, R.J., Henley, R.W., 1976. Dewatering of a metamorphic pile. Geology 4, 333–336.
O'Neil, J.R., Taylor, H.P., 1967. The oxygen isotope and cation exchange chemistry of feldspars. Am. Mineral. 52, 1414–1437.
O'Neil, J.R., Taylor, H.P., 1969. Oxygen isotope equilibrium between muscovite and water. J. Geophys. Res. 74, 6012–6022.
Pitcairn, I.K., Teagle, D.A.H., Craw, D., Olivio, G.R., Kerrich, R., Brewer, T.S., 2006. Sources of metals and fluids in orogenic gold deposits: insights from the Otago and Alpine Schists, New Zealand. Econ. Geol. 101, 1525–1546.
Purdie, H., Berter, N., MacKintosh, A., Baker, J., Rhodes, R., 2010. Isotopic and elemental changes in winter snow accumulation on glaciers in the Southern Alps of New Zealand. J. Climate 23, 4737–4749.
Raimondo, T., Clark, C., Hand, M., Cliff, J., Anczkiewicz, R., 2013. A simple mechanism for mid-crustal shear zones to record surface-derived fluid signatures. Geology 41, 711–714.
Raimondo, T., Clark, C., Hand, M., Faure, K., 2011. Assessing the geochemical and tectonic impacts of fluid–rock interaction in mid-crustal shear zones: a case study from the intracontinental Alice springs orogen, central Australia. J. Metamorph. Geol. 29, 821–850.
Reyes, A.G., Christenson, B.W., Faure, K., 2010. Sources of solutes and heat in low-enthalpy mineral waters and their relation to tectonic setting, New Zealand. J. Volcanol. Geotherm. Res. 192, 117–141.
Reynolds, S.J., Lister, G.S., 1987. Structural aspects of fluid–rock interactions in detachment zones. Geology 15, 362–366.
Sharp, Z.D., 1990. A laser-based microanalytical method for the in situ determination of oxygen isotope ratios in silicates and oxides. Geochim. Cosmochim. Acta 54, 1353–1357.
Shi, Y., Allis, R., Davey, F., 1996. Thermal modeling of the Southern Alps, New Zealand. Pure Appl. Geophys. 146, 469–501.
Sibson, R.H., 1981. Controls on low-stress hydro-fracture dilatancy in thrust, wrench and normal-fault terrains. Nature 289, 665–667.
Sibson, R.H., 1992a. Fault-valve behavior and the hydrostatic–lithostatic fluid pressure interface. Earth-Sci. Rev. 32, 141–144.
Sibson, R.H., 1992b. Implications of fault-valve behaviour for rupture nucleation and recurrence. Tectonophysics 211, 283–293.
Stern, T., Okaya, D., Kleffman, S., Scherwath, M., Henrys, S., Davey, F., 2007. Geophysical exploration and dynamics of the Alpine Fault zone. In: Okaya, D., Stern, T., Davey, F. (Eds.), A Continental Plate Boundary, Tectonics at South Island, New Zealand. In: Geophysical Monograph, vol. 175. American Geophysical Union, Washington, DC, pp. 207–233.
Stewart, M.K., Cox, M.A., James, M.R., Lyon, G.L., 1983. Deuterium in New Zealand rivers and streams. DSIR, Lower Hutt, Institute of Nuclear Sciences. Institute of Nuclear Sciences IN-S-320. 42 p.
Stockhert, B., Brix, M.R., Kleinschrodt, R., Hurford, A.J., Wirth, R., 1999. Thermochronometry and microstructures of quartz-a comparison with experimental flow laws and predictions on the temperature of the brittle–plastic transition. J. Struct. Geol. 21, 351–369.
Sutherland, R., 1999. Cenozoic bending of New Zealand basement terranes and Alpine Fault displacement: a brief review. N.Z. J. Geol. Geophys. 42, 295–301.
Sutherland, R., Toy, V.G., Townend, J., Cox, S.C., Eccles, J.D., Faulkner, D.R., Prior, D.J., Norris, R.J., Mariani, E., Boulton, C., Carpenter, B.M., Menzies, C.D., Little, T.A., Hasting, M., De Pascale, G.P., Langridge, R.M., Scott, H.R., Reid-Lindroos, Z., Fleming, B., Kopf, A.J., 2012. Drilling reveals fluid control on architecture and rupture of the Alpine Fault, New Zealand. Geology 40, 1143–1146.
Suzuki, S., Nakashima, S., 1999. In-situ IR measurements of OH species in quartz at high temperatures. Phys. Chem. Miner. 26, 217–225.
Suzuoki, T., Epstein, S., 1976. Hydrogen isotope fractionation between OH-bearing minerals and water. Geochim. Cosmochim. Acta 40, 1229–1240.
Taylor, H.P., 1974. The application of oxygen and hydrogen isotope studies to problems of hydrothermal alteration and ore deposition. Econ. Geol. 69, 843–883.
Taylor, H.P., 1977. Water/rock interactions and the origin of H_2O in granitic batholiths: thirtieth William Smith lecture. J. Geol. Soc. 133, 509–558.
Teagle, D.A.H., Hall, C.M., Cox, S.C., Craw, D., 1998. Ar/Ar dating and uplift rate of hydrothermal minerals in the Southern Alps, New Zealand. Water–Rock Int. 9, 801–804.

Templeton, A.S., Chamberlain, C.P., Koons, P.O., Craw, D., 1998. Stable isotopic evidence for mixing between metamorphic fluids and surface-derived waters during recent uplift of the Southern Alps, New Zealand. Earth Planet. Sci. Lett. 154, 73–92.

Toy, V.G., Craw, D., Cooper, A.F., Norris, R.J., 2010. Thermal regime in the central Alpine Fault zone, New Zealand: constraints from microstructures, biotite chemistry and fluid inclusion data. Tectonophysics 485, 178–192.

Upton, P., Craw, D., Caldwell, T.G., Koons, P.O., James, Z., Wannamaker, P.E., Jiracek, G.J., Chamberlain, C.P., 2003. Upper crustal fluid flow in the outboard region of the Southern Alps, New Zealand. Geofluids 3, 1–12.

Upton, P., Koons, P.O., Chamberlain, C.P., 1995. Penetration of deformation-driven meteoric water into ductile rocks: isotopic and model observations from the Southern Alps, New Zealand. N.Z. J. Geol. Geophys. 38, 535–543.

Vry, J.K., Storkey, A.C., Harris, C., 2001. Role of fluids in the metamorphism of the Alpine Fault Zone, New Zealand. J. Metamorph. Geol. 19, 21–31.

Walther, J.V., Orville, P.M., 1982. Volatile production and transport in regional metamorphism. Contrib. Mineral. Petrol. 79, 252–257.

Wannamaker, P.E., Jiracek, G.R., Stodt, J.A., Caldwell, T.G., Gonzalez, V.M., McKnight, J.D., Porter, A.D., 2002. Fluid generation and pathways beneath an active compressional orogen, the New Zealand Southern Alps, inferred from magnetotelluric data. J. Geophys. Res. 107, 1–20.

Warr, L.N., Cox, S.C., 2001. Clay mineral transformations and weakening mechanisms along the Alpine Fault, New Zealand. Geol. Soc. (Lond.) Spec. Publ. 186, 85–101.

Weatherley, D., Henley, R.W., 2013. Flash vaporization during earthquakes evidenced by gold deposits. Nat. Geosci. 6, 294–298.

Wenner, D.B., Taylor, H.P., 1971. Temperatures of serpentinization of ultramafic rocks based on $^{18}O/^{16}O$ fractionation between coexisting serpentine and magnetite. Contrib. Mineral. Petrol. 32, 165–185.

Wightman, R.H., Little, T.A., 2007. Deformation of the Pacific Plate above the Alpine Fault Ramp and its relationship to expulsion of metamorphic fluids: an array of backshears. In: Okaya, D., Stern, T., Davey, F. (Eds.), A Continental Plate Boundary: Tectonics at South Island, New Zealand. In: Geophysical Monograph, vol. 175. American Geophysical Union, Washington, DC, pp. 177–205.

Wightman, R.H., Prior, D.J., Little, T.A., 2006. Quartz veins deformed by diffusion creep-accommodated grain boundary sliding during a transient, high strain-rate event in the Southern Alps, New Zealand. J. Struct. Geol. 28, 902–918.

Wintsch, R.P., Christoffersen, R., Kronenberg, A.K., 1995. Fluid–rock reaction weakening of fault zones. J. Geophys. Res., Solid Earth 100, 13021–13032.

Woods, R., Hendrikx, J., Henderson, R., Tait, A., 2006. Estimating mean flow of New Zealand rivers. J. Hydrol. 45, 95–109.

Yardley, B.W.D., 1997. The evolution of fluids through the metamorphic cycle. In: Jamtveit, B., Yardley, B.W.D. (Eds.), Fluid Flow and Transport in Rocks: Mechanisms and Effects. Chapham and Hall, London, pp. 99–121.

Yardley, B.W., 2009. The role of water in the evolution of the continental crust. J. Geol. Soc. 166, 585–600.

Zheng, Y.F., 1993a. Calculation of oxygen isotope fractionation in anhydrous silicate minerals. Geochim. Cosmochim. Acta 57, 1057–1091.

Zheng, Y.F., 1993b. Calculation of oxygen isotope fractionation in hydroxyl-bearing silicates. Earth Planet. Sci. Lett. 120, 247–263.